Infrared Spectroscopic Determination of Lactide Concentration in Polylactide: An Improved Methodology

Birgit Braun,[†] John R. Dorgan,*[,†] and Steven F. Dec[‡]

Departments of Chemical Engineering and Chemistry, Colorado School of Mines, Golden, Colorado 80401

Received August 19, 2006; Revised Manuscript Received October 23, 2006

ABSTRACT: In this study, a new Fourier transform infrared (FTIR) spectroscopy method for measuring lactide concentration in a polylactide (PLA) matrix is presented. The lactide ring breathing mode peak at 935 cm^{-1} is rationed against the asymmetric bending mode of methyl groups at 1454 cm^{-1}; because the methyl group is present both in lactide monomer and the polymer, this ratio provides a direct measure of lactide concentration. Using well-defined mixtures of lactide and PLA, a calibration curve is established. For lactide concentrations corresponding to conversions above 75%, a linear relationship between conversion and the peak area ratio exists. Below 75% conversion, the development of a double peak at 1454 cm^{-1} leads to deviations from linearity; data can then be accurately represented by a second-order polynomial relating conversion to the peak area ratio. Kinetic data for the bulk polymerization of lactide at different temperatures are also obtained and independently verified using rigorous NMR techniques. Finally, conversion as a function of time calculated using the FTIR method is found to be in good agreement with the polymerization kinetics model of Witzke, Narayan, and Kolstad.

Introduction

Most polymeric materials currently in use for packaging applications are based on nonrenewable and increasingly expensive petroleum. When disposed of after their short life span, they contribute to escalating demands on land devoted to solid waste disposal, and the valuable resources embedded in the polymeric structure are lost. In addition, plastics manufacture and incineration for energy recovery produce CO_2, and therefore contribute to global warming. In recent years, these pressing environmental concerns have resulted in increasing attention being paid to biodegradable polymeric materials based on renewable resources.

Polylactide (PLA) is an aliphatic polyester derived from renewable resources, such as corn, sugar beets, and cheese whey, and it is ultimately degradable under compositing conditions. Its mechanical properties make it useful for fibers, packaging, and other applications traditionally dominated by petroleum-based resins. A life cycle analysis performed by Vink et al. on the large-scale PLA production employed by NatureWorks (Minnetonka, MN) showed that it has a significantly lower non-renewable-energy content compared to various other common polymers partly due to the elimination of fossil fuels for its monomer source.[1]

PLA is most widely synthesized through ring-opening polymerization of lactide, the cyclic dimer of lactic acid, which was first demonstrated by Carothers, Dorough, and Van Natta in 1932.[2] Tin 2-ethylhexanoate (tin octoate, or $Sn(Oct)_2$) is commonly used as a catalyst due to its ability to produce PLA in relatively short time periods with high conversion and low racemization up to 180 °C. This catalyst has also been approved by the Food and Drug Administration for food contact,[3] making it ideal for many packaging applications.

Thermophysical properties of polymers show a dependence on molecular weight before plateauing above some critical molecular weight. However, the presence of residual monomer in the polymeric matrix can serve as plasticizer, lowering mechanical strength and thermal stability. In the case of PLA, lactide monomer remaining in the final product can also decrease shelf life. During processing, large amounts of residual monomer can cause problems such as changes in viscosity and rheological behavior, as well as fuming.[3] Accordingly, rapid and reliable analytical methods for determining lactide concentrations in PLA are of interest from both a scientific and commercial perspective. Frequently used analytical methods for determining residual lactide concentration in PLA include: gel permeation chromatography (GPC),[4−6] polarimetry,[4−6] nuclear magnetic resonance (NMR),[7−11] or simple gravimetric means after precipitation of the polymer. [12−14] The last method can result in a systematic error associated with the calculated conversion, since oligomers and low molecular weight polymeric chains often show some solubility in the non-solvent for the polymer. Extraction of the residual monomer followed by gas chromatography is also documented in the literature.[15] A few studies discuss the use of Fourier transform infrared spectroscopy (FTIR) for lactide conversion analysis;[6,17] however, the strategies employed are not based on sound physical concepts. Degée et al. used the ratio of the absorbance of the peak at 935 cm^{-1} to the absorbance at 1383 cm^{-1} to establish a calibration plot independent of the absolute sample concentration. This calibration curve was subsequently used to analyze lactide conversion during reactive extrusion as a function of time.[16] However, the reported functional relationship between the absorbance ratio and conversion was simply fit to a fifth order polynomial. Such an approach can be improved upon using the correlations expected from the simple theoretical considerations outlined below.

The advantages of using FTIR for conversion analysis are numerous and include high sensitivity as well as low cost. In addition, instrumentation is readily available allowing on-line measurements during film processing as well as in situ monitoring of polymerization reactions in conjunction with a remote attenuated total reflectance (ATR) probe.[17] These techniques

* Author to whom correspondence should be addressed. E-mail: jdorgan@mines.edu.
[†] Department of Chemical Engineering, Colorado School of Mines.
[‡] Department of Chemistry, Colorado School of Mines.

10.1021/ma061922a CCC: $33.50
Published on Web 12/08/2006

enable rapid measurements without the necessity of materials sampling and are therefore ideal for on-line process control. Usually FTIR is used in laboratories for compound identification, since quantitative analysis is often nontrivial, requiring clean sample material and thorough data evaluation.[18] In this study, a new methodology is presented in order to enable better utilization of the many advantages of FTIR in determining residual monomer content.

Materials and Methods

A. Materials. L-Lactide and polylactide (Natureworks 2000D) used in this study were purchased from NatureWorks (Minnetonka, MN). The weight-average molecular weight of the PLA was determined to be about 170 000 g/mol by intrinsic viscosity measurements.[19] L-Lactide was recrystallized from ethyl acetate. Prior to the use in standard blends for FTIR analysis, PLA was purified by dropwise addition of solutions in chloroform (0.04 g/mL) into a 10-fold excess of chilled methanol followed by drying under vacuum (25 mmHg) at 60 °C overnight.

B. Polymerizations. The ring-opening polymerization of lactide was performed in a Haake Rheomix 600 at 180 or 200 °C, and catalyzed by stannous octoate, $Sn(Oct)_2$, which was obtained from Sigma Aldrich and used as received. The catalyst concentration in all experiments was $R = 2500$ monomer molecules per catalyst molecule. Tris(nonyl phenyl phosphite) (TNPP) is known to serve as a stabilizer for PLA,[20] and was shown to have no adverse effects when added prior to polymerization.[21] TNPP was purchased from Sigma Aldrich and added at a concentration of 0.5 wt % with respect to the initial mass of lactide. For handling purposes, solutions of the catalyst and the stabilizer were prepared in anhydrous toluene.

C. FTIR. Films of blends of PLA (P) and lactide (L), denoted P/L, or samples taken at various reaction times during the bulk polymerization of lactide, were cast onto KBr pellets (IR grade from Sigma Aldrich) from solutions in chloroform (concentration of 0.04 g/mL), and the solvent was allowed to evaporate at room temperature for at least 3 h prior to measurement. No evidence of residual solvent was observed spectroscopically. Spectra were recorded on a Thermo Nicolet Nexus 670 FTIR in the range 400−4000 cm^{-1}. The instrument settings were kept constant (120 scans; data spacing, 0.964 cm^{-1}; velocity, 0.6329; aperture, 69).

D. NMR. Kinetics samples from polymerization reactions were dissolved in deuterated chloroform, and ^1H NMR spectra recorded on a Chemagnetics CMX Infinity 400 Solids/Liquids NMR spectrometer. A tetramethylsilane (TMS) signal was used as the zero chemical shift reference.

E. Peak Area Calculation. Absorption peak areas were determined using the software package Omnic 6.0 according to the so-called baseline method.[22] In this method, a straight line was established between two fixed points on the spectra insensitive to composition located at wavenumbers below and above the peaks of interest. Peak areas were also calculated by fitting the absorbance signals with Gaussian peaks using Origin 7.5 Pro software to ensure the validity of the numerical peak area calculation integrated in the Omnic software. The data followed the same trend, proving that the use of the Omnic spectrometer software provides accurate results.

Theory

Beer's law is the basis of quantitative analysis using infrared spectroscopy. This relationship relates the absorbance of infrared light of a specific wavelength, $a(\lambda)$, to the properties of the material through which the light is traveling. It states that absorbance equals the product of the sample thickness l [cm], the concentration of the vibrating bond in the sample c [mol L^{-1}] and the molar absorptivity $e(\lambda)$ [L cm^{-1} mol^{-1}], a wavelength specific material constant.

$$a(\lambda) = lce(\lambda) \tag{1}$$

At high concentrations of the absorbing bond, deviations from Beer's law can be observed. The critical concentration for the deviation from a linear relationship between the absorbance and concentration depends on the substance of interest and its physical form. Also, if the material is highly scattering, deviations are more likely to be observed at lower concentrations.[22]

When Beer's law is obeyed, quantitative analysis is commonly carried out by the establishment of a calibration curve relating the absorbance at a characteristic wavenumber to the concentration of the compound of interest. In a binary mixture, the absolute concentration dependence of the absorption can be eliminated in certain cases. This is possible when the intensity at a characteristic wavelength for one component can be normalized by the signal at a wavenumber shared by both compounds. This allows a more accurate analysis of solid materials by exclusion of the experimental error induced through changing sample thicknesses.

In the specific case of PLA/lactide mixtures, the absorbance at a wavelength characteristic of the monomer (λ_1) to the absorbance at a wavelength shared by the polymer and monomer (λ_2) is computed by making use of eq 1 to give

$$\frac{a(\lambda_1)}{a(\lambda_2)} = \frac{c_{L,\lambda_1} e(L,\lambda_1)}{c_{P,\lambda_2} e(P,\lambda_2) + c_{L,\lambda_2} e(L,\lambda_2)} \tag{2}$$

In eq 2 it is the molar concentrations of functional groups (i.e., chemical bonds) on the lactide, c_{L,λ_1}, and polymer, c_{P,λ_1}, that are being counted. Substitution into eq 2 in terms of the total concentration c_{TOT} provides,

$$\frac{a(\lambda_1)}{a(\lambda_2)} = Z_{P/L} = \frac{w_L c_{TOT} e(L,\lambda_1)}{w_P c_{TOT} e(P,\lambda_2) + w_L c_{TOT} e(L,\lambda_2)} \tag{3}$$

where the weight fractions of PLA, w_P, and lactide, w_L, are used because the molecular weights of the monomer and the polymer repeat unit are identical. For polymerization, the conversion X, is defined by eq 4.

$$X = \frac{w_P}{w_P + w_L} \tag{4}$$

Using this definition to eliminate the weight fractions in eq 3 yields the useful result relating the ratio of absorbances to the conversion given in eq 5.

$$Z_{P/L} = \frac{e(L,\lambda_1)}{\left(\frac{X}{1-X}\right) e(P,\lambda_2) + e(L,\lambda_2)} \tag{5}$$

Rearrangement of eq 5 leads to the conclusion that a linear relationship must exist between $X/(1 - X)$ and the inverse of the absorbance ratio, $1/Z_{P/L}$, at λ_1 and λ_2 as shown in eq 6.

$$\left(\frac{X}{1-X}\right) = \frac{e(L,\lambda_1)}{e(P,\lambda_2)}\left(\frac{1}{Z_{P/L}}\right) - \frac{e(L,\lambda_2)}{e(P,\lambda_2)} \tag{6}$$

For this to be true, a careful selection of the peaks employed in the conversion calculation is crucial. Even then, structural effects such as hydrogen bonding or changes in the short range molecular arrangements, may alter the position and shape of absorbance peaks[23] thereby affecting the accuracy of the analysis. Equation 6 is referred to as the "general case" in this

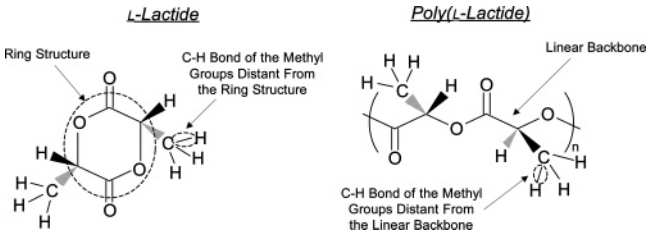

Figure 1. Structures of L-lactide and PLA depicting the fundamental differences between the monomer and polymer. In NMR analysis, the methine peaks (C−H) are well separated for lactide (5.03 ppm) and PLA (5.16 ppm) allowing conversion analysis based on peak area integration. The same is true for the methyl signals ($C-H_3$) for lactide (1.59 ppm) and PLA (1.69 ppm).

paper; a number of limiting cases of eq 6 are of general interest and are now discussed.

I. $X = 0$. This case corresponds to FTIR analysis being performed on a pure lactide sample, and allows the computation of the ratio of absorptivities of the two functional groups of interest at the wavenumbers considered, $e(L,\lambda_1)/e(L,\lambda_2)$.

II. $e(L,\lambda_2) = e(P,\lambda_2)$ [$=e(\lambda_2)$]. If the absorptivities of the two components at the shared normalization wavelength are equal, a simplified relation between the conversion X and the ratio of the peak intensities $Z_{P/L}$ can be derived. The significance of this case, as well as the validity of its underlying assumption, is discussed later in the paper.

$$X = 1 - \frac{e(\lambda_2)}{e(L,\lambda_1)} Z_{P/L} \tag{7}$$

III. $X \rightarrow 1$: This is an interesting case from an industrial perspective, since the concentration of residual lactide for sufficient material properties is well below 10 wt %, corresponding to conversions of $X = 0.9$ and above. As X advances toward 1, the ratio $X/(1 - X)$ approaches infinity. From this, it can be assumed that the second term in the denominator in eq 5 is negligible compared to the first, and rearrangement leads to a linear relationship between $(1/X)$ and the peak ratio $Z_{P/L}$ given by eq 8.

$$\left(\frac{1}{X}\right) = \frac{e(P,\lambda_2)}{e(L,\lambda_1)} Z_{P/L} + 1 \tag{8}$$

In this study, all three special cases are examined by spectral analysis of defined PLA/lactide mixtures, and then tested by various means for their accuracy with respect to conversion analysis during lactide polymerization.

Results and Discussion

The most important task for successful conversion analysis using FTIR is the selection of the peaks employed in the analysis for monomer determination and normalization. The chemical structures of the lactide monomer and PLA polymer are depicted in Figure 1. There is a significant difference between monomer and polymer because lactide processes a ring structure. Therefore, distinct absorption bands associated with only the ring structure are exceptionally suitable for monomer detection. Normalization requires infrared bands originating from both compounds. The C−H bonds of the methyl groups are well separated from the lactide ring structure and PLA linear backbone structure. Accordingly, infrared signals from the methyl C−H bonds should be appropriate to normalize the lactide signal and allow accurate conversion analysis.

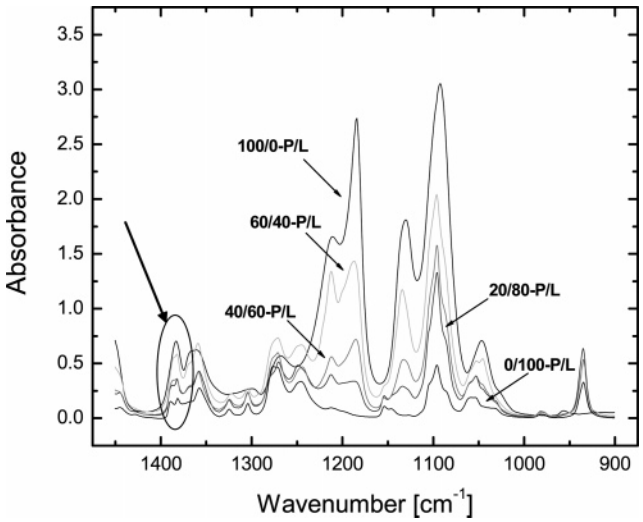

Figure 2. Fingerprint region of spectra obtained from samples containing various fractions of PLA and lactide (60/40-P/L corresponds to 60% PLA and 40% lactide based on total mass). Note the changes in the peak centered at 1383 cm^{-1}.

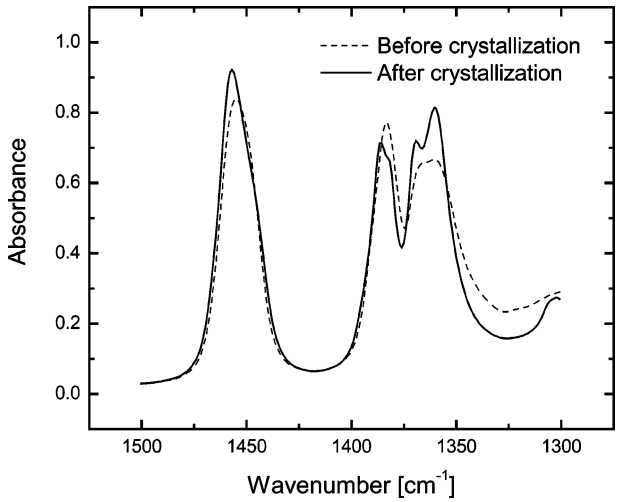

Figure 3. Spectra in the region between 1520 and 1320 cm^{-1} for pure PLA (100/0-P/L) before and after crystallization at 110 °C for 16 h.

From an examination of the fingerprint region of spectra obtained from samples containing various fractions of lactide and PLA (shown in Figure 2), it is apparent that the presence of lactide can be clearly monitored in the mid-IR region by an isolated peak at a wavenumber of 935 cm^{-1}. This band is assigned to the COO ring breathing mode.[16] The signal used by Degée et al.[16] to normalize the lactide absorbance is assigned to the symmetric $C-H_3$ deformation mode[24] at 1383 cm^{-1} and is common to lactide and PLA. However, the peak is not isolated and overlaps with at least two other bands, namely the first overtone of the C−H bending vibration and the symmetric bending vibration of $C-H_3$ group.[24] In addition, the 1383 cm^{-1} peak splits into two bands with increasing concentrations of lactide leading to the complete disappearance of the peak for pure lactide accompanied by the appearance of peaks centered at 1389 and 1381 cm^{-1}. Also, the peak centered at 1383 cm^{-1} exhibits some sensitivity toward the ordering of the polymer chains. Figure 3 shows the region between 1500 and 1320 cm^{-1} of spectra obtained before and after crystallization of PLA at 110 °C for 16 h, and the development of a shoulder peak at lower wavenumbers can be observed. Factor group splitting is known to occur in semicrystalline polyethylene and attributed to an increased order among polymer chains, sometimes

correlated to crystallinity.[23] However, only few polymers exhibit pronounced factor group splitting since it is very sensitive to the separation of chains in the unit cell, and the chains are simply too far apart in most semicrystalline polymers to result in strong enough intermolecular forces showing crystal field splitting in the spectrum.[18] Zhang et al.[25] as well as Sarasua et al.[26] concluded from melt-crystallization studies that weak interchain interactions among the $C-H_3$ groups in the unit cell of crystalline PLLA in the α polymorph are responsible for some observed correlation field splitting of $C-H_3$ bands in PLA. However, the presence of hydrogen bonding of C═O and $C-H_3$ side groups between PLA chains was ruled out as the origin for the documented observation.[27,28] Due to the presence of strongly absorbing bonds in close proximity as well as its sensitivity to crystallinity, it is not recommended to use the band at 1393 cm^{-1} as an internal standard for conversion analysis.

Messman and Storey used the absorbance of the peak at 1240 cm^{-1} associated with the C−O−C ring stretch to follow the progress of lactide polymerization using FTIR in conjunction with a remote attenuated total reflectance (ATR) probe for real-time monitoring.[17] However, they point out that overlapping polymer absorbances at 1185 cm^{-1} (asymmetric C−O−C stretching vibration and asymmetric $C-H_3$ rocking vibration[24]) and 1270 cm^{-1} (bending vibration of C−H and C−O−C stretching vibration[24]) lead to an overestimation of the absorbance at 1240 cm^{-1}. In addition, this peak is in close proximity to the C−C ring stretching vibration which is observed in the region of 1275−1245 cm^{-1}.[29] As a limitation, the method employed by these authors only allows monitoring the progress of a specific reaction since no internal normalization of the monomer signal was performed.

The peak centered at 1454 cm^{-1} is assigned to the $C-H_3$ asymmetric bending mode and is known to be a suitable internal standard.[24] It is used for normalization of the characteristic lactide peak at 935 cm^{-1} in this study due to its isolated position in the infrared spectra of both PLA and lactide. Upon crystallization, the 1454 cm^{-1} band only shows a small high-wavenumber shift and intensity increase as documented in Figure 3. Consistent with Figure 3, Zhang et al. investigated the cold crystallization behavior of PLA and found that the 1454 cm^{-1} peak exhibits some sensitivity to the extent of short-range order in the polymer.[30]

Second derivative spectra are useful in resolving closely overlapping bands, and a comparison between pure PLA and two prepared standard blends of PLA and lactide is presented in Figure 4. The derivatives of the peak for PLA and the 75/25-P/L blend show the presence of two bands. The signal at 1458 cm^{-1} results from a phase exhibiting short-range order among the PLA chains. As the amount of lactide in the sample increases (25/75-P/L), the peaks shift slightly toward lower wavenumbers, corresponding to the doublet observed in pure lactide. This could be an indication that the interaction of PLA chains is reduced by the presence of lactide in the blends. Nevertheless, the overall effect of PLA crystallinity on the peak position and shape is minor.

As shown in Figure 5, splitting of the single $C-H_3$ bending mode into two peaks is again observed to a significant extent at higher lactide concentrations. The decreasing intensity of the peak signal is likely to be caused by scattering effects due to the crystalline lactide fraction in the sample. Another possible explanation for this observation could be a significant difference of the molar absorptivities of PLA and lactide at this wavelength; however, this can be ruled out by experimental findings discussed later in the paper. Despite some sensitivity toward

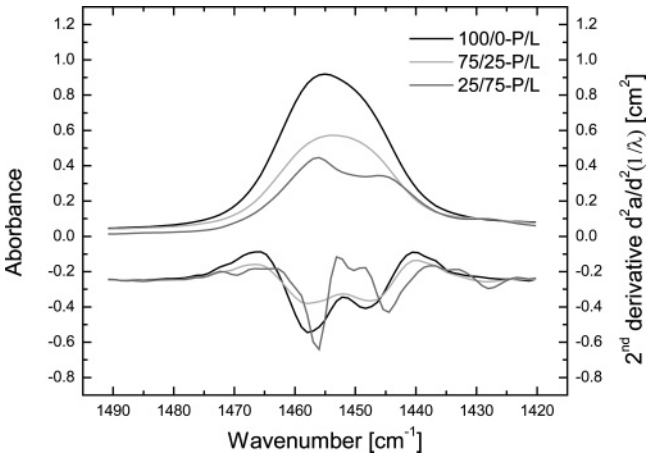

Figure 4. Second derivative spectra of the $C-H_3$ bending mode centered at 1454 cm^{-1} for pure PLA (100/0-P/L) and two blends of PLA and lactide (75/25-P/L and 25/75-P/L). Second derivative spectra are amplified and shifted ($20I_0 - 0.25$) for better visualization.

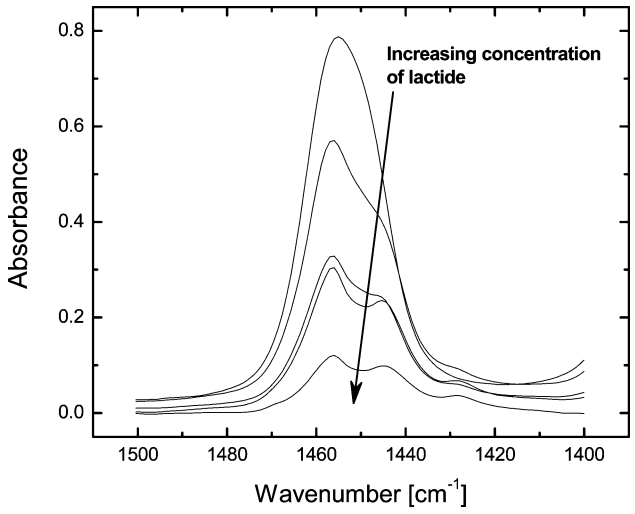

Figure 5. Spectral region between 1520 and 1400 cm^{-1} showing the formation of a double peak of medium intensity with increasing lactide concentration in a binary blend of lactide and PLA accompanied by a decrease in absorbance. Infrared spectra are shown for 100/0-P/L, 60/40-P/L, 40/60-P/L, 20/80-P/L, and 0/100-P/L.

short-range order of $C-H_3$ groups and the development of a double band at higher lactide concentrations, the band centered at 1454 cm^{-1} is a good choice for the internal normalization standard due to its isolated position and the fact that both effects are minor in the range of lactide concentrations of predominant interest ($X \geq 0.75$). Accordingly, this band is adopted in the new methodology proposed by this work.

In order to establish a calibration curve, peak areas of the band centered at 935 cm^{-1} for defined blends of PLA and lactide were calculated between the limits of 946 and 920 cm^{-1} with a straight baseline established between 967 and 905 cm^{-1}. Areas under the 1454 cm^{-1} peak were measured between 1480 and 1432 cm^{-1} with a straight baseline from 1500 to 1410 cm^{-1}. According to eq 6, the resulting data are used to construct a plot of $X/(1 - X)$ vs the inverse of the peak area ratio $1/Z_{P/L}$ for conversions ranging from $X = 0$ to $X = 1$ as shown in Figure 6. The data follow the predicted linear trend very well for PLA fractions up to 0.97, but deviates for higher conversions. This observation is partly caused by drastically increasing uncertainties in the exact blend composition. The last two data points ($X = 0.98$ and 0.99) were therefore not included in the linear fit that provided the relationship $X/(1 - X) = A + B/Z_{P/L}$ with

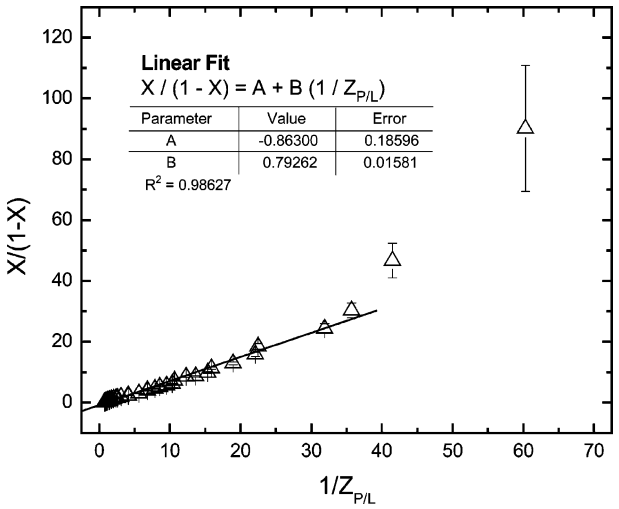

Figure 6. Plot of $X/(1 - X)$ vs $1/Z_{P/L}$ for defined blends of PLA and lactide. The concentration of lactide corresponds to conversions ranging from $X = 0$ to $X = 1$.

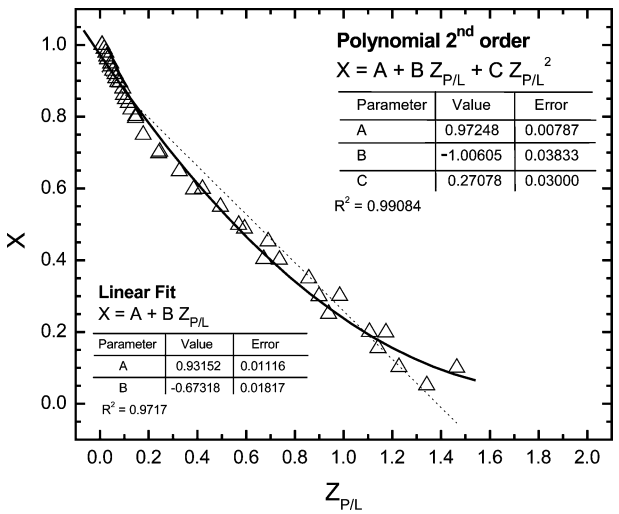

Figure 7. Conversion X vs peak area ratio $Z_{P/L}$ for blends of lactide concentrations corresponding to the entire range of conversion ($0 \leq X \leq 1$) for special case II (assuming equal molar absorptivities of the C−H_3 bending mode for PLA and lactide).

$A = -0.863 \pm 0.18596$ and $B = 0.79262 \pm 0.01581$ and $R^2 = 0.986$. The accuracy of the linear fit for lactide determination was examined and is discussed in a later section.

Special Case I: $X = 0$. From multiple spectra recorded from pure lactide samples, the average peak area ratio $Z_{0/100}$ was determined to be 1.427 ± 0.175. Structural considerations (six C−H methyl bonds per lactide ring) lead to the experimental estimation of the absorptivity ratio of the lactide ring breathing mode to the C−H asymmetric bending mode of the methyl groups, e(L,935)/e(L,1454), of 8.562 ± 1.049.

Special Case II: $e(L,\lambda_2) = e(P,\lambda_2)$. The intercept of the linear fit for the general case (conversions below $X = 0.98$) was found to be -0.863 ± 0.18596. According to eq 6, this value equals the negative of the ratio of the absorptivities for the C−H_3 bending mode of PLA to lactide. It is not surprising that the ratio is close to one, since the bending vibration of the C−H bonds of the methyl groups are expected to give rise to bands of similar intensity, independent of whether they are attached to a ring structure or a polymer backbone. The assumption underlying special case II therefore seems to be valid, and eq 7 should provide a reasonable approximation. Figure 7 is a graph of the conversion vs the peak area ratio covering the entire range from 0 to 100% PLA. At higher lactide concentration a deviation from linearity is again encountered so that the overall correlation is better represented by a second-order polynomial. The inconsistency of the data with the expected functional relation is probably caused by the observation discussed earlier, namely the appearance of a double peak at lower conversions. At lactide concentrations less than 25%, corresponding to 75% monomer conversion, the influence of the peak splitting is insignificant and an excellent agreement is found between measurements of defined standard blends and the expected linear relationship between conversion X and the peak area ratio; this is shown in Figure 8.

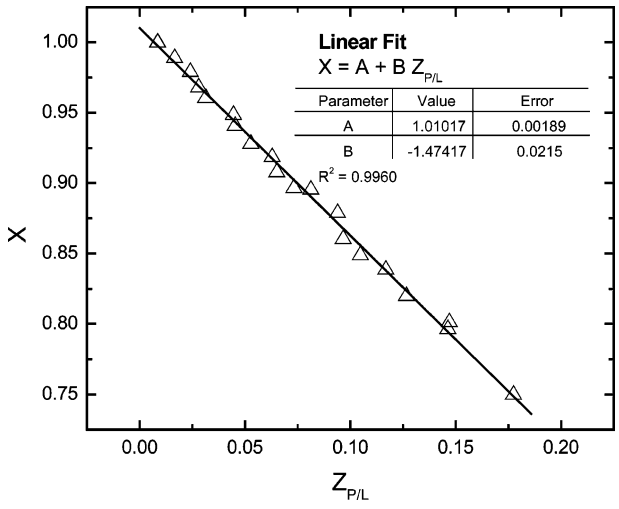

Figure 8. Conversion X vs peak area ratio $Z_{P/L}$ at high conversions [$X \geq 0.75$] according to special case II (assuming equal absorptivities of the C−H_3 bending modes for PLA and lactide).

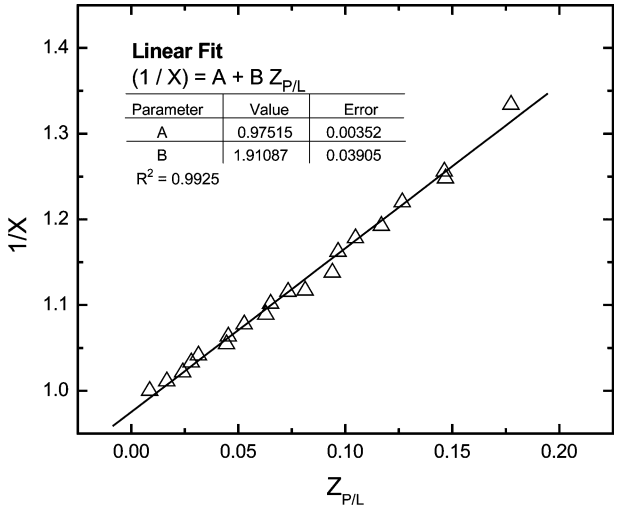

Figure 9. Inverse of conversion ($1/X$) plotted as a function of the peak area ratio $Z_{P/L}$ for conversions greater than $X \geq 0.75$ according to special case III.

Special Case III: $X \rightarrow 1$. Since the range of predominant interest for conversion analysis involves lactide concentrations of 10 wt % or less, the approximation of a dominating first term in the denominator of eq 5 should be applicable for most cases. At $X = 0.75$ and assuming equal absorptivity of the CH_3 bending mode in lactide and PLA, the first term in the denominator of eq 5 is about 3 times higher than the second term with a rapid increase in value as the conversion approaches 1. Figure 9 shows the inverse of conversion $1/X$ as a function of the peak area ratio for conversions greater than 75%; it is evident that an excellent linear relationship is present.

Table 1. Absorptivity Ratios Estimated from Experimental Data

	L-ring/P-methyl e(L,935)/e(P,1454)		L-methyl/P-methyl e(L,935)/e(P,1454)		L-ring/L-methyl e(L,935)/e(P,1454)	
	ratio	error	ratio	error	ratio	error
general case, linear	4.7557	0.2902	0.8630	0.0158	5.5107	0.2397
special case I					8.5620	1.0490
special case II, linear					4.0701	0.0585
special case III, linear	3.1399	0.0629				

The absorptivity ratios estimated from fitting the experimental data of defined PLA/lactide blends to the various functional relationships derived earlier, are summarized in Table 1. There is a significant variation among the values determined from the fits to the general case and the special cases. The most accurate values are obtained from the general case fit. As mentioned previously, the estimated value of the absorptivity ratio for e(L,1454)/e(P,1454) = 0.863 ± 0.0158 shows that the approximation leading to special case II (assuming equal absorptivities for the C−H methyl bending mode for PLA and lactide) is reasonable.

The accuracy of the calibrated method was tested in three ways. First, PLA/lactide blends of known compositions were measured and analyzed using the calibration curves resulting from the general case and special case II and III. Second, conversion data obtained by FTIR were also compared to NMR measurements preformed on samples taken at various reaction times during the bulk polymerization of L-lactide in our laboratory to ensure the applicability of the calibration to PLA samples obtained from a non-commercial source. Finally, the data are compared to the theoretical model describing the reversible kinetics of the homopolymerization of L-lactide with stannous octoate developed by Witzke, Narayan, and Kolstad.[15] The results of the three tests are summarized below.

Table 2 contains the comparison between lactide concentrations analyzed by FTIR with the known composition of defined blends. At the two higher conversions, 90% and 94%, all calibration curves except the polynomial fit to special case II give results corresponding well with the known lactide concentration (i.e., lie within the experimental error of the method). However, the deviation encountered using the polynomial fit of special case II for the 94% conversion sample is small. Analysis of the sample containing a higher concentration of lactide (45%) leads to the finding that only the polynomial fit gives a result within good agreement; however, the error associated with it is fairly significant (13.4%).

Figure 10 shows an example of a typical ^{1}H NMR spectrum for samples obtained at various reaction times during the bulk polymerization of lactide. Conversion of the monomer can be calculated from the relative peak areas of the monomer and polymer methine quartet at 5.03 and 5.16 ppm ($A_{CH,L}$ and $A_{CH,P}$) or the methyl doublets at 1.59 and 1.69 ppm ($A_{CH_3,L}$ and $A_{CH_3,P}$) as shown in eqs 9 and 10.

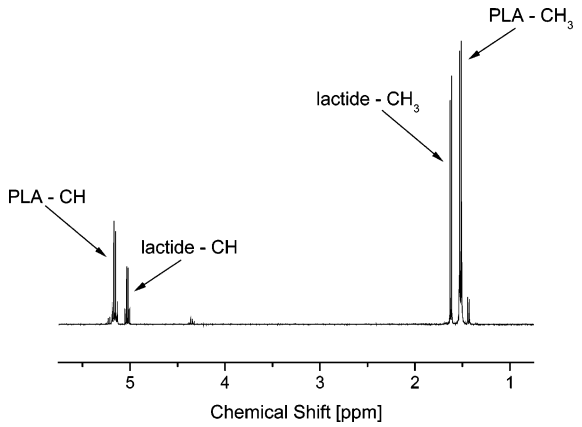

Figure 10. ^{1}H NMR spectrum of a bulk sample dissolved in deuterated chloroform obtained after a polymerization time of 5 min at 200 °C using $Sn(Oct)_2$ as catalyst in the presence of TNPP as stabilizer.

$$X_{CH}(t) = \frac{A_{CH,P}}{A_{CH,P} + A_{CH,L}} \tag{9}$$

$$X_{CH_3}(t) = \frac{A_{CH_3,P}}{A_{CH_3,P} + A_{CH_3,L}} \tag{10}$$

Table 2 allows direct comparison of the conversion kinetics data obtained by FTIR with NMR results. Similar to the tests using defined blends, only the polynomial fit of special case II gives consistently good results for conversions lower than 75%. At conversions $X \geq 0.75$, NMR data lie within the experimental error of conversion data calculated using the linear fits according to special cases II and III.

The overall best performance with regards to accuracy of conversion analysis using FTIR is achieved by using a combination of the polynomial fit, for conversions between 0% and 75%, and the special case II linear fit, for conversions above 75%. In addition to the highest accuracy, the simplicity of the equations (directly relating the conversion X with the peak area ratio $Z_{P/L}$) makes these the preferred choices for data analysis based on the experimental findings.

The Witkze model describing the kinetics of conversion during bulk polymerization of lactide consists of the following three equations:[15]

$$X(t) = \left(1 - \frac{M_{eq}}{M_0}\right)[1 - \exp(-k_p It)] \tag{11}$$

$$M_{eq} = \exp\left(\frac{\Delta H_{lc}}{RT} - \frac{\Delta S_{lc}}{R}\right) \tag{12}$$

$$k_p = A_{448} \exp\left[-\frac{E_a}{R}\left(\frac{1}{T} - \frac{1}{448}\right)\right] \tag{13}$$

In eq 11, $X(t)$ is the conversion at a given time, t [h], and I is the initiator concentration [(h cat mol %)$^{-1}$]. Initiation is assumed to be fast compared to polymerization, and the concentration of chain initiating species is set equal to the catalyst concentration. M_{eq} is the equilibrium concentration of lactide in the polymeric matrix as defined in eq 12. ΔH_{lc} and ΔS_{lc} are the heat and entropy of polymerization at equilibrium between pure monomer liquid, l, and condensed amorphous polymer, c ($\Delta H_{lc} = -23.3 \pm 1.5$ kJ/mol, $\Delta S_{lc} = -22.0 \pm 3.2$ J/mol). k_p is the propagation rate constant, and it is described by an Arrhenius relationship given by eq 13, where $E_a = -70.9 \pm 1.5$ kJ/mol is the activation energy, and $A_{448} = 86.0 \pm 3.0$ (h cat mol %)$^{-1}$ is the pre-exponential constant at the reference temperature of 448 K. R and T are the gas constant (8.314 J/(mol K)) and temperature in kelvin, respectively.

Table 2. Comparison of Lactide Concentration Determined by FTIR (Expressed as Conversion *X*) Using the Various Calibration Curves Established with the Known Composition of the Samples, or Results from NMR Analysis

Standard PLA/Lactide Blends

		general case linear		special case II				special case III linear	
				polynominal		linear			
no.	known	*X*	error	*X*	error	*X*	error	*X*	error
1	0.5500	0.4095	0.1016	0.5304	0.0713	0.2610	0.0999	0.5133	0.0359
2	0.9000	0.9065	0.0165	0.8985	0.0192	0.8995	0.0163	0.8940	0.0185
3	0.9400	0.9390	0.0108	0.9240	0.0153	0.9382	0.0113	0.9360	0.0142

	general case linear	special case II		special case III linear
		polynominal	linear	
all *X* (%)	66.67	66.67	66.67	66.67
$X < 0.75$ (%)	0.00	100.00	0.00	0.00
$X > 0.75$ (%)	100.00	50.00	100.00	100.00

Kinetics of Lactide Conversion Compared to NMR

		general case linear		special case II				special case III linear	
				polynominal		linear			
t (min)	NMR	*X*	error	*X*	error	*X*	error	*X*	error
				R2500/200C/100rpm					
5	0.7174	0.7050	0.0515	0.7434	0.0421	0.6509	0.0488	0.6940	0.0323
10	0.8618	0.8830	0.0206	0.8801	0.0219	0.8713	0.0200	0.8657	0.0210
20	0.9358	0.9388	0.0108	0.9239	0.0153	0.9380	0.0113	0.9357	0.0143
40	0.9511	0.9415	0.0103	0.9260	0.0150	0.9412	0.0109	0.9394	0.0139
60		0.9467	0.0094	0.9302	0.0144	0.9475	0.0101	0.9466	0.0131
90		0.9423	0.0102	0.9266	0.0149	0.9422	0.0108	0.9405	0.0138
				R2500/180C/25rpm/0.5TNPP					
5	0.3607	0.1423	0.1456	0.3582	0.0918	-0.1255	0.1502	0.4086	0.0341
10	0.7613	0.6952	0.0532	0.7361	0.0432	0.6385	0.0504	0.6864	0.0326
20	0.8667	0.8499	0.0211	0.8777	0.0223	0.8675	0.0205	0.8620	0.0214
40	0.9499	0.9415	0.0103	0.9261	0.0150	0.9413	0.0109	0.9395	0.0139
60	0.9587	0.9501	0.0088	0.9329	0.0139	0.9515	0.0096	0.9513	0.0126
94		0.9561	0.0077	0.9376	0.0132	0.9586	0.0086	0.9597	0.0116
112		0.9557	0.0078	0.9373	0.0133	0.9581	0.0087	0.9591	0.0117

	general case linear	special case II		special case III linear
		polynominal	linear	
all *X* (%)	66.67	66.67	66.67	77.78
$X < 0.75$ (%)	33.33	100.00	0.00	33.33
$X > 0.75$ (%)	83.33	50.00	100.00	100.00

Overall Agreement

	general case linear	special case II		special case III linear
		polynominal	linear	
all *X* (%)	66.67	66.67	66.67	75.00
$X < 0.75$ (%)	25.00	100.00	0.00	25.00
$X > 0.75$ (%)	87.50	50.00	100.00	100.00

Debate about the nature of this chain initiating species can be found in the literature;[7,31−34] however, it has been clearly demonstrated that tin octoate merely serves as catalyst and is not the chain initiating species. Instead, tin alkanoates formed by reaction of the tin 2-ethylhexanoic acid with hydroxyl group containing species initiate the reaction. The assumption integrated in the model is that the catalyst-activating species (containing hydroxyl groups) is present in excess in the reaction mixture. In the case of the polymerization of lactide in the Haake and the use of tin octoate as received (95% purity on a weight basis with the remaining 5% consisting of octanoic acid and water), it is highly probable that this assumption of excess initiating groups is valid.

Figure 11 depicts conversion vs reaction time for bulk polymerization of lactide at 180 °C at a catalyst level of $R = 2500$ mol of lactide/mol of catalyst analyzed by FTIR and NMR. Also included in the plot is the reversible kinetics model by Witzke, Narayan, and Kolstad for the experimental parameters. Conversions analyzed by FTIR and NMR are in good agreement, and the progress of lactide consumption as a function of time follows the trend predicted by the model. The slight deviation at early reaction times is likely caused by the presence of the stabilizing agent (TNPP) used in this study, resulting in slightly higher conversion compared to the model prediction. The equilibrium lactide concentrations in the samples however are in perfect agreement with the predicted values from the Witzke model.

The conversion kinetics at 200 °C with catalyst present at the same level ($R = 2500$) is shown in Figure 12, also including the model prediction. Excellent agreement is again found for the equilibrium concentration of lactide at reaction times longer than 30 min, and the experimental data as determined by FTIR and verified by NMR follow the model closely. The effect of the stabilizer is less pronounced which can be attributed to the higher reaction temperature resulting in a more rapid consumption of the TNPP, and therefore a less significant stabilization effect is observed.

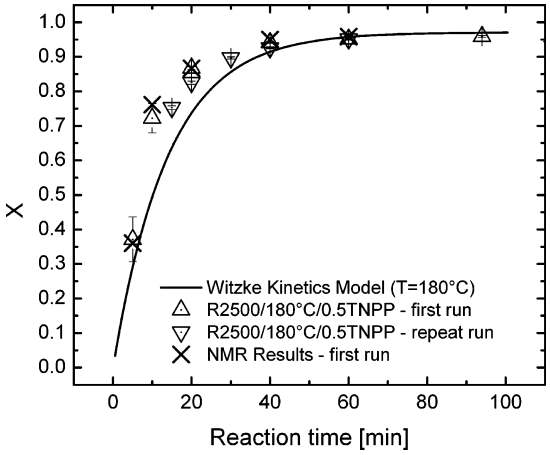

Figure 11. Conversion as a function of reaction time for lactide polymerization at 180 °C analyzed by FTIR and NMR plotted with the prediction from Witzke kinetics model.

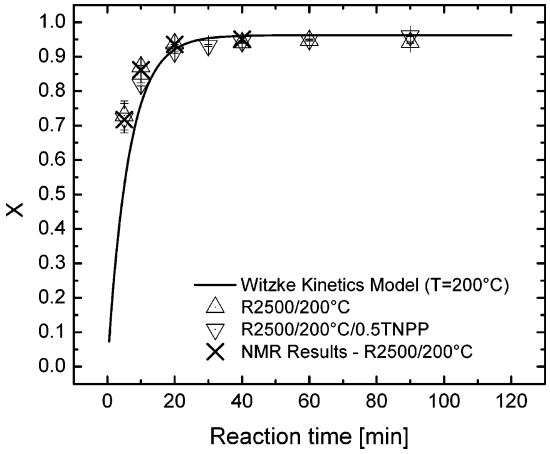

Figure 12. Conversion as a function of reaction time for lactide polymerization at 200 °C analyzed by FTIR and NMR plotted together with the prediction from Witzke kinetics model.

Conclusions

In this study, a new approach to the evaluation of infrared spectroscopic data of PLA/lactide blends was developed. The method allows accurate determination of the lactide fraction in the mixture, and can therefore be used as a tool in conversion analysis of PLA polymerization reactions or to determine lactide content during film and fiber processing operations. FTIR is an attractive methodology for in situ studies and on-line process control.

The functional relationship relating conversion, X, and the area ratio between a spectroscopic peak characteristic for the monomer to a band originating from both the polymer and its monomer is derivable based on physical ideas. The resulting expressions are readily applicable to other monomer/polymer systems and only require a careful selection of the peaks involved in the analysis. For the lactide/polylactide system, the optimal peaks to employ are the COO ring breathing mode for the monomer at 935 cm^{-1} and the methyl bending mode centered at 1454 cm^{-1} for normalization. The 1454 cm^{-1} peak is chosen due to its isolated position in the spectrum and low sensitivity toward short range order at high conversions. Very good agreement is found between experimental data on defined blends of known composition and the expected functional relationship for conversions up to 97%.

Two special cases for the establishment of a calibration curve arise from the general model. One is based on the assumption of equal molar absorptivities of the methyl bending mode for PLA and lactide. This is a reasonable assumption based on the experimentally determined value of 0.863 ± 0.186 for the ratio of the absorptivities. Experimental data follow the resulting linear prediction between conversion, X, and the peak area ratio, $Z_{P/L}$, in an excellent manner for lactide fractions between 0 and 0.25, corresponding to conversions of 75% and higher. At lower conversions, a second-order polynomial gives a good representation of the experimental data. The second special case describes the limiting situation of high lactide conversion for which a linear relationship between the inverse of conversion $1/X$ and the peak area ratio $1/Z_{P/L}$ is derived. Again, good agreement between experiment and prediction is found. On the basis of these findings, suitable expressions are now available to determine lactide concentrations throughout the entire binary compositional range.

Conversion results for blends of known composition and polymerization kinetic samples determined by FTIR using the general function relation and the two special cases are compared to the PLA fraction known, or NMR analysis. Kinetic behavior is examined using the theoretical model described by Witzke, Narayan, and Kolstad where GC−MS methods were used for its calibration. It was found that a combination of the polynomial fit (for conversions X less than 75%) and the linear fit (for higher conversions) relating X directly with the peak area ratio $Z_{P/L}$ gives the most accurate results. In industrial applications, where the range of predominant interest is at high conversions, this method should be of considerable practical utility.

Acknowledgment. The authors gratefully acknowledge funding support from the EPA and NSF under the Technologies for a Sustainable Environment Program, Grant No. RD83153001.

References and Notes

(1) Vink, E. T. H.; et al. *Polym. Degrad. Stab.* **2003**, *80*, 403−419.
(2) Carothers, W. H.; Dorough, G. L.; Van, Natta, F. J. *J. Am. Chem. Soc.* **1932**, *54*, 761−772.
(3) Hartmann, M. H. High Molecular Weight Polylactic Acid Polymers. In *Biopolymers from Renewable Resources*; Kaplan, D. H., Ed.; Springer-Verlag: Berlin, 1998; pp 367−411.
(4) Kowalski, A.; et al. *Macromolecules* **2000**, *33*, 1964−1971.
(5) Kowalski, A.; Duda, A.; Penczek, S. *Macromolecules* **1998**, *31*, 2114−2122.
(6) Kowalski, A.; Duda, A.; Penczek, S. *Macromolecules* **2000**, *33*, 7359−7370.
(7) Nijenhuis, A. J.; Grijpma, D. W.; Pennings, A. J. *Macromolecules* **1992**, *25*, 6419−6424.
(8) Li, S.; et al. *Polym. Degrad. Stab.* **2001**, *71*, 61−67.
(9) Stridsberg, K.; Albertsson, A.-C. *J. Polym. Sci.: Part A: Polym. Chem.* **2000**, *38*, 1774−1784.
(10) Thakur, K. A. M.; Munson, E. J.; Kean, R. T. *Macromolecules* **1997**, *30*, 2422.
(11) Du, Y. J.; et al. *Macromolecules* **1995**, *28*, 2124−2132.
(12) Zhu, K. J.; Xiangzhou, L.; Shilin, Y. *J. Appl. Polym. Sci.* **1990**, *39*, 1−9.
(13) Kricheldorf, H. R.; Damrau, D.-O. *Macromol. Chem. Phys.* **1998**, *199*(8), 1747−1752.
(14) Kricheldorf, H. R.; Damrau, D.-O. *Macromol. Chem. Phys.* **1997**, *198*, 1753−1766.
(15) Witzke, D. R.; Narayan, R.; Kolstad, J. J. *Macromolecules* **1997**, *30*, 7075−7085.
(16) Degee, P.; et al. *J. Polym. Sci.: Part A: Polym. Chem.* **1999**, *37*, 2413−2420.
(17) Messman, J. M.; Storey, R. F. *J. Polym. Sci.: Part A: Polym. Chem.* **2004**, *42*, 6238−6247.
(18) Koenig, J. L. *Spectroscopy of Polymers*; ACS Professional Reference Book; American Chemical Society: Washington, DC, 1992.
(19) Dorgan, J. R.; et al. *J. Polym. Sci.: Part B: Polym. Phys.* **2005**, *43*, 3100−3111.
(20) Cicero, J. A.; et al. *Polym. Degrad. Stab.* **2002**, *78*, 95−105.
(21) Kolstad, J. J.; et al. US Patent 6,353,086, 2000 (Cargill, Inc.).
(22) Brügel, W. *An Introduction to Infrared Spectroscopy*, 2nd ed.; John Wiley & Sons Inc.: London and New York, 1962.

(23) Lagaron, J.-M. *Macromol. Symp.* **2002**, *184*, 19−36.
(24) Kister, G.; Cassanas, G.; Vert, M. *Polymer* **1998**, *39* (2), 267−272.
(25) Zhang, J.; et al. *J. Phys. Chem. B* **2004**, *108*, 11514−11520.
(26) Sarasua, J.-R.; et al. *Macromolecules* **2005**, *38*, 8362−8371.
(27) Zhang, J.; et al. *J. Mol. Struct.* **2005**, *735*−736., 249−257.
(28) Meaurio, E.; et al. *J. Phys. Chem.* B **2006**, *110*, 5790−5800.
(29) Kister, G.; et al. *Eur. Polym. J.* **1992**, *28* (10), 1273−1277.
(30) Zhang, J.; et al. *Macromolecules* **2004**, *37*, 6433−6439.
(31) Kricheldorf, H. R.; Kreiser-Saunders, I.; Boettcher, C. *Polymer* **1995**, *36*, 1253−1259.
(32) Kowalski, A.; Duda, A.; Penczek, S. *Macromol. Rapid Commun.* **1998**, *19*, 567−572.
(33) Kowalski, A.; Duda, A.; Penczek, S. *Macromolecules* **2000**, *33*, 689−695.
(34) Zhang, X.; et al. *J. Polym. Sci.: Part A: Polym. Chem.* **1994**, *32*, 2965−2970.

MA061922A